GROWTH OF ZINC OXIDE NANOSTRUCTURES

USING CHEMICAL METHODS

by

Tiffany L. Denny

A thesis submitted to the Faculty of the University of Delaware in partial fulfillment of the requirements for the degree of Master of Science in Electrical and Computer Engineering.

Winter 2006

UMI Number: 1432295

UMI Microform 1432295

ProQuest Information and Learning Company
300 North Zeeb Road
P.O. Box 1346
Ann Arbor, MI 48106-1346

GROWTH OF ZINC OXIDE NANOSTRUCTURES

USING CHEMICAL METHODS

by

Tiffany L. Denny

Approved: _____
Olufemi Olowolafe, Ph.D.
Professor in charge of thesis on behalf of the Advisory Committee

Approved: _____
Robert L. Opila, Ph.D.
Professor in charge of thesis on behalf of the Advisory Committee

Approved: _____
Gonzalo R. Arce, Ph.D.
Chair of the Department of Electrical and Computer Engineering

Approved: _____
Eric W. Kaler, Ph.D.
Dean of the College of Engineering

Approved: _____
Conrado M. Gempesaw II, Ph.D.
Vice Provost for Academic and International Programs

ACKNOWLEDGMENTS

I wish to thank my advisors, Dr. Olufemi Olowolafe and Dr. Robert Opila, Dr. Opila's research group and Dr. Prather's research Group.

I must also thank my mother, Sheila Perks, without whom none of this would ever have been possible; and my best friends, Michelle, Cortney, Fallon and Tyreef.

I also wish to thank Dean Michael Vaughan, NSF, and the Bridges to the Doctorate students who have supported me in every way.

TABLE OF CONTENTS

LIST OF TABLES v
LIST OF FIGURES vi
ABSTRACT ix

Chapter

1 INTRODUCTION 1

1.1 Zinc Oxide Properties and Applications 1
1.2 Electrodeposition 2
1.3 Wet Chemistry 5
1.4 Application of Current Work 7

2 EXPERIMENTAL 8

2.1 Electrodeposition 8
2.2 Wet Chemistry 9
2.3 Analysis 11

2.3.1 Scanning Electron Microscopy 11
2.3.2 Symmetric X-Ray Diffraction 11

3 RESULTS AND DISCUSSION 13

3.1 Electrodeposition 13
3.2 Wet Chemistry 28

4 CONCLUSION AND FUTURE WORK 45

4.1 Conclusion 45
4.2 Future Work 47

BIBLIOGRAPHY 50

LIST OF TABLES

Table 1.1 Table on the Progression of Semiconductors. 4

Table 2.1 Parameters for Electrodeposition Experiments 9

Table 2.2 Parameters for Wet Chemistry Experiments. 10

LIST OF FIGURES

Figure 1.1 Sketch of an Electrodeposition System 3

Figure 3.1 Sample 01 has hexagonal ZnO platelets approximately 3000 nm in diameter. Growth conditions were 0.05 M $ZnCl_2$, 67°C, -0.7V SCE, 60 minutes on Au substrate. 14

Figure 3.2 Sample 07 has hexagonal ZnO platelets approximately 2000 nm in diameter. Growth conditions were 0.05 M $ZnCl_2$, 67-70°C, -0.7V SCE, and 45 minutes on Au substrate. 15

Figure 3.3 Sample 06, in cross section has hexagonal ZnO platelets approximately 3000 nm in diameter Growth conditions were 0.05 M $ZnCl_2$, 67°C, -0.7V SCE, 20 minutes on Au substrate. 17

Figure 3.4 Hexagonal ZnO platelets approximately 2400 nm in diameter. Growth conditions were 0.05 M $ZnCl_2$, 67°C, -0.7V SCE, 70 minutes on Au substrate. 18

Figure 3.5 Cross sectional view of sample. Growth conditions were 0.05M $ZnCl_2$, 67-70º C, -0.6V SCE, and 20 minutes on Au substrate. 20

Figure 3.6 Depicted are actual dimensions of ZnO platelets ranging from 1320nm-2070nm in diameter. Growth conditions were 0.025M $ZnCl_2$, 67-70º C, -0.7V SCE for 20 minutes on Au substrate. 21

Figure 3.7 ZnO platelets vary in diameter. Growth conditions were 0.025M $ZnCl_2$, 67-70º C, -0.7V SCE for 45 minutes on Au substrate. 22

Figure 3.8 ZnO platelets are clustered together. Growth conditions were 0.025M $ZnCl_2$, 67-70º C, -0.6V SCE for 20 minutes on Au substrate. 23

Figure 3.9 ZnO platelets, grown randomly, are approximately 3μm in diameter. Growth conditions were 0.02M $ZnCl_2$, 67-70º C, -0.7V SCE for 20 minutes. 25

Figure 3.10 The beginning growth of ZnO nanostructures. Growth conditions were 0.02M $ZnCl_2$, 70º C, -0.7V SCE for 5 minutes on Au substrate. 26

Figure 3.11 ZnO platelets, 13 μm in diameter, nucleate into the surface of the substrate. Growth condition were 0.02M $ZnCl_2$, 67º C, -0.8V SCE for 20 minutes on Au substrate. 27

Figure 3.12 ZnO cluster of nanorods. Growth conditions were equimolar 0.02M concentration, 65ºC for 120 minutes on Au substrate. 29

Figure 3.13 ZnO cluster of nanorods, about 300nm in diameter. Growth conditions were 0.02M solution, 65º C for 180 minutes on Au substrate. 30

Figure 3.14 ZnO random distorted growth. Growth conditions were 0.02M, >80º C for 120 minutes on Au substrate. 31

Figure 3.15 ZnO rods shown with slight distortion. Growth conditions were 0.02M, 75º C for 120 minutes on Au substrate. 32

Figure 3.16 ZnO rods approximately 1.5 μm in diameter. Growth conditions were 0.02M, 75º C for 75 minutes on Al substrate. 34

Figure 3.17 ZnO rods ranging from 500nm – 1 μm in diameter. Growth conditions were 0.02M, 75º C for 65 minutes on Al substrate. 35

Figure 3.18 ZnO platelets, 500nm in diameter. Growth conditions were 0.1M, 65º C for 75 minutes 36

Figure 3.19 ZnO platelet structures 500nm in diameter. Growth conditions were 0.02M, 65º C for 120 minutes on Al substrate. 37

Figure 3.20 A few ZnO rods are visible, but there is a lot of nucleation and growth. Growth conditions were 0.02M, > 80º C for 75 minutes on Al substrate. 38

Figure 3.21 ZnO nanorods, about 100-200 nm, are growing along the (0001) plane outward from the surface. Growth conditions were 0.02M, 55º C and 75 minutes on Ag substrate. 40

Figure 3.22 ZnO nanorods, approximately 100nm in diameter, grow parallel to the surface. Larger ZnO rods nucleate together. Growth conditions were 0.02M, 65º C for 75 minutes on Ag substrate. 41

Figure 3.23 ZnO nanorods, 200nm in diameter, grow along the (0001) plane. Growth conditions were 0.02M, 75º C for 75 minutes on Ag substrate 42

Figure 3.24 ZnO nanorods, 200nm in diameter, grow along the (0001) plane. Growth conditions were 0.02M, 75º C for 75 minutes on Ag substrate. 43

Figure 3.25 Symmetric XRD of ZnO Wet Chemistry Sample 016 44

Figure 4.1 Schematic of future work using a two point probe..... 49

ABSTRACT

Zinc oxide is a group II-VI n-type semiconductor with a band gap of approximately 3.3-3.6 eV. The purpose of this research was to deposit and grow ZnO nanorod structures on suitable substrates. Two deposition methods, electrodeposition and wet chemistry, were investigated. In both methods, variables such as solution concentration, deposition time, temperature and substrate were changed so that the optimal recipe could be realized. Analysis was completed by using scanning electron microscopy (SEM) and symmetric x-ray diffraction (XRD) to determine the structure and morphology of the surface. Both deposition methods allowed for the growth of ZnO. Electrodeposition resulted in hexagonal ZnO platelet structures, ranging in 1000-3000 nm in diameter on Au substrates. Variation in growth times from 20-70 minutes did not effect growth; the potential -0.6V SCE resulted in poor growth, but potential ≥ -0.7V/SCE resulted in good growth. The growth appeared to be caused by the electric field concentration of the platelet's edges. Using wet chemistry, optimal growth was found on a Ag substrate, which produced ZnO nanorods approximately 200 nm in diameter and less than 1μm in length growing along the (0001) plane.

CHAPTER 1

INTRODUCTION

1.1 Zinc Oxide and Applications

Zinc Oxide is an n-type semiconductor material with a wide band gap of 3.3-3.6 eV. It has various unique properties such as a high exciton binding energy (60mV), high breakdown strength, absorption of UV light, resistance to radiation, luminescence characteristics and piezoelectric. ZnO is optimal for such applications as high frequency devices, chemical sensors, solar cells, UV detectors, surface acoustic wave (SAW) devices, UV light emitting devices and piezoelectric devices. This semiconductor material also has other interesting properties such as ferroelectricity and ferromagnetism [1].

A bulk of the ZnO research focuses on ZnO nanostructures. Nanorod and other nano-sized structures are attractive because many of them can be integrated onto a single chip, and will be important in nano-size electronic, optical, sensor and optoelectronic devices. Several groups report on the nanoring structure of ZnO [2, 3, 4]. At the Georgia Institute of Technology, physicists were able to grow single crystal ZnO nanorings by using a solid-vapour method. ZnO nanorings, approximately 1 - 4 μm in diameter and shells about 10 – 30 nm thick were deposited onto a silicon substrate. It is believed that these nanorings structures will

be useful for such applications as, fabricating piezoelectric based fluid pumps and switches for the biotechnology industry or micro-electromechanical systems (MEMS).

Another group reported on ZnO UV nanowire lasers, which were grown on a sapphire substrate [5]. Once grown, the ZnO nanowires were synthesized by a vapor process and laser cavities, 20 – 150 nm in diameter and about 10 μm in length, were created. These structures may be useful for applications that use short wavelength semiconductor lasers.

In recent developments of ZnO, many groups have demonstrated growth of ZnO nanorods [6-12]. D. P. Norton et al. reviews the growth, doping and fabrication processes for ZnO and realizes that nanorods have a large surface area, which makes them useful for gas and chemical sensing. For nanorods to function as sensors, it will be important to control the lateral and longitudinal composition to realize the heterostructures. Mg doping was used to help create the ZnO nanorods, which resulted in a lateral heterojunction. Controlling these dimensions to smaller sizes than obtainable through photolithography may be used to produce faster devices that use very little power.

1.2 Electrodeposition

Electrodeposition is a method in which a substance is deposited onto an electrode. When a voltage is applied, current passes through the electrolyte which contains ions, thus allowing the ions to follow the electric field. The positive ions will then adsorb at the negatively charged cathode. At the cathode, reduction takes place while oxidation takes place at the anode, therefore a redox reaction occurs. In general, the reduction reaction follows the chemical equation $M^{z+} + ze^- \rightarrow M$. Shown below is a picture of a typical electrodeposition system and each component.

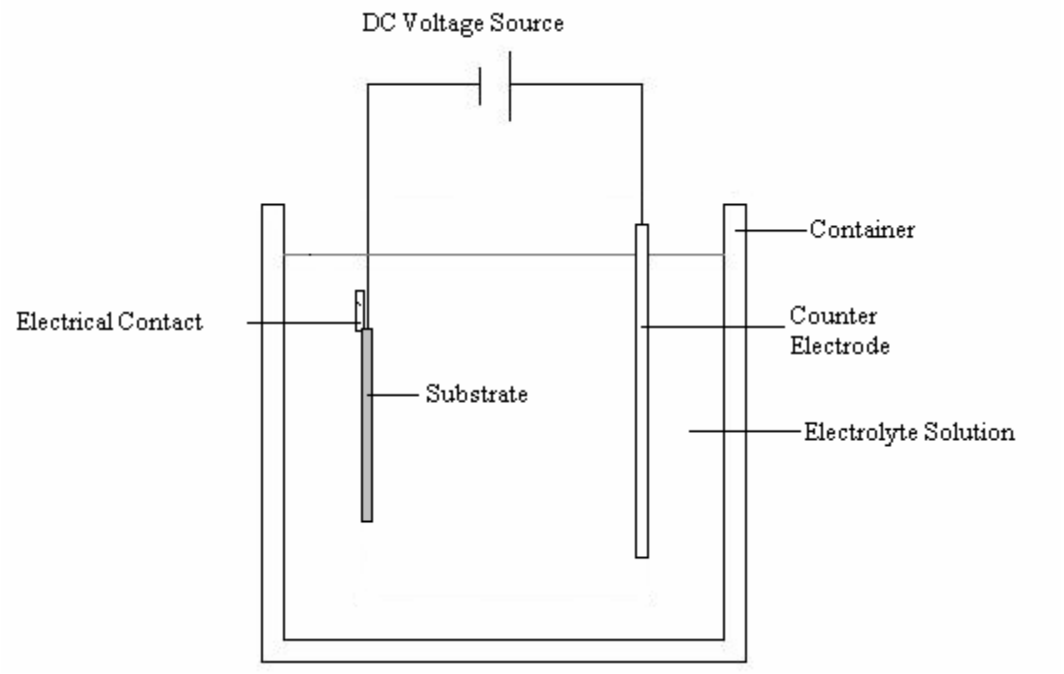

Figure 1.1 Sketch of an Electrodeposition System

Electrodeposition of semiconductors is a process that has been used for many years for depositing thin films and nanostructures. Lincot designed a roadmap that shows the progression over time of the electrodeposition for many semiconductors. It shows that ZnO is one of the newest materials being electrodeposited since approximately 1996 [13].

Table 1.1 Table on the Progression of Semiconductors

Semiconductor	Year Research Began	Year of Most Research Intensity
Si	1865	1976
Ge	1886	1949
GaP	1968	1978
InP	1981	1983
GaAs	1978	1982
CdS	1980	2000
CdSe	1963	1985
CdTe	1928	1995-2000
$CuInSe_2$	1983	2000
ZnO	**1996**	**2000-**

Many researchers have ventured into the study of electrodeposited zinc oxide. The motivation for the research later described comes from a few of these researchers. Cathodic electrodeposition of ZnO was explored by S. Peulon and D. Lincot [9]. An aqueous solution comprised of $ZnCl_2$ and supporting electrolyte KCl, along with bubbling oxygen/argon gas is used, which shows quality ZnO films deposited. Studies show that electrodeposition, as well as control of the layer

morphology of the ZnO. The principle behind their research is that dissolved oxygen can be used as the source to synthesize oxides. Further experiments also show there will not be film deposition without the presence of oxygen in the solution.

Izaki and Omi show that transparent ZnO films can also be cathodically deposited using an aqueous solution containing 0.1 M zinc nitrate at 335K (62 ºC) [7]. The experiment results in various surface morphologies, as well as deposition rate, dependent on the cathodic potential. They were able to show that the optical transmission increases as the potential increases from -1.5V (V vs. Ag/AgCl) to -1.0V, but then begins to decrease as the potential increases to -0.5V.

Switzer et al. explored the epitaxial electrodeposition of ZnO and was able to grow ZnO nanopillars by using an aqueous solution containing $ZnCl_2$ and KCl [8]. The hypothesis behind his research is the large lattice mismatch (-20.3%) between ZnO and the substrate, Gold, allows for the growth of 3 dimensional structures. Results for these experiments included ZnO pillars with a diameter of 85 nm on the Au (111) and Au (110) surface and 95 nm on the Au (100) surface.

1.3 Wet Chemistry

Wet chemistry involves chemistry which occurs in water or an aqueous solution; it differs from electrodeposition in that it does not use nor rely on electricity for deposition of the substance. The lab setup is similar to the setup for

electrodeposition, except there is no applied voltage, nor any electrodes; there is a solid substrate, upon which ZnO deposits nucleate.

Using a wet chemistry method to deposit ZnO has previously been researched. Vayssiers et al. [11] reports on the growth of 3 dimensional oriented microrod array of ZnO by using an aqueous precursor in a solution. He believes that the shape and orientation of crystallites can be controlled by observing the thermodynamics, nucleation and growth. In Vayssiers' experiment, synthesis is based on the aqueous thermal decomposition of Zn^{2+} amino complex. Aqueous solution consisted of 0.1M of zinc nitrate ($Zn(NO_3)_2)\cdot 4H_20$) and 0.1M of methenamine, $C_6H_{12}N_4$ in a stopped flask placed in an oven. Substrates were a Si or SiO_2 wafer, or a bare piece of glass on conductive plastic; it is noted that the crystal structure of these substrates does not influence the ZnO nanorod growth. The results obtained from this experiment were an array of ZnO hexagonal rods about 1μm in diameter, growing along the (001) direction and perpendicular to the surface of the substrate.

Julia W.P. Hsu et al reports on the direct spatial organization of Zinc Oxide nanorods [10]. Self-Assembled Monolayers (SAM) were used as templates to direct the nucleation of the ZnO. The aqueous solution consisted of 0.02M zinc nitrate and 0.02M of hexamethylenetetramine (HMT), $C_6H_{12}N_4$. Selectivity, nucleation density, crystal orientation and spatial organization of ZnO nanorods are

controlled; and ZnO nucleation is inhibited on the SAM sections of the substrate. Results included approximately 46 ± 6 crystals per 2 μm diameter nucleation site.

1.4 Application of Current Work

Once ZnO nanorods are grown, the next step is to deposit a thin insulating layer of SiO_2 onto the substrate; Plasma Enhanced Chemical Vapor Deposition (PECVD) is the method by which this is done. Following SiO_2 deposition is the etching of holes through the SiO_2 to make an electrical contact with any of the ZnO nanorods by using a Focused Ion Beam (FIB). Next, a 2-point probe system will be applied to make a contact on both ends of the nanorod (see Figure 4.1). Thus, the electrical properties can be examined; for example, the voltage can be varied and the current observed. The ultimate goal is to measure the electrical properties discovered from these nanostructures and construct an electronic device that incorporates these properties.

CHAPTER 2

EXPERIMENTAL

2.1 Electrodeposition

Electrodeposition was carried out using a solution containing 99.99% pure 5 X 10^{-2} M $ZnCl_2$ and 0.1M of supporting electrolyte 99.99% KCl (Alfa Aesar, used without further purification). Pure distilled H_2O was utilized. Oxygen gas (Keen) is bubbled through the solution at a constant rate throughout the duration of deposition. The substrate/working electrode is approximately 100nm thick single crystal gold evaporated onto freshly cleaved mica. The substrate is kept in an air tight sample holder until ready for use; it was not rinsed before deposition. The Auxiliary electrode is platinum gauze and the reference electrode is mercury/mercury chloride calomel. A potentiostat, Princeton Applied Research (PAR) 263A, using a typical three-electrode electrodeposition setup is used for application of potential and to monitor the current changes.

Various experiments, parameters shown below in Table 2.1, were performed changing one variable i.e. deposition time, solution concentration or potential, so that the optimal recipe can be determined.

Table 2.1 Parameters for Electrodeposition Experiments

Sample	Potential (V vs. SCE)	Temperature (ºC)	Deposition Time (minutes)	Current (A)	$ZnCl_2$ Concentration (M)
01	-0.7 V	67º	60 min	0.03 → 0.0	0.05 M
06	-0.7 V	67º	20 min	0.028 → 0.006	0.05 M
07	-0.7 V	67º	45 min	0.04 → 0.008	0.05 M
08	-0.7 V	67º	70 min	0.04 → 0.01	0.05 M
09	-0.6 V	67º	20 min	0.046 → 0.0	0.05 M
10	-0.7 V	67º	20 min	0.056 → 0.015	0.025 M
11	-0.7 V	67º	45 min	0.056 → 0.015	0.025 M
12	-0.6 V	67º	20 min	0.055 → 0.015	0.025 M
14	-0.7 V	67º	15 min	0.04 → 0.01	0.02 M
15	-0.7 V	67º	5 min	0.04	0.02 M
18	-0.8 V	67º	20 min	0.06 → 0.05	0.02 M

At the end of each experiment, the sample is rinsed in DI water, applied from a plastic container, and air dried at room temperature.

2.2 Wet Chemistry

The wet chemistry deposition is carried out using an aqueous equimolar solution containing zinc nitrate, [$(Zn(NO_3))_2$, Alfa Aesar 99.99% pure], and methenamine, $C_6H_{12}N_4$ (Alfa Aesar, 99+% pure), used without further purification. The water was 18 MΩ resistant H_2O. The substrates used for these experiments consisted of either 1000 Å thick single crystal Au evaporated onto a Silicon wafer, with a thin Cr adhesion layer between the Au and the Si as an adhesive layer; 1000

Å thick Al evaporated onto a Si wafer or 1000 Å silver e-beam evaporated onto a Si wafer. A covered beaker containing the solution is placed in a water bath, to control the temperature on a hotplate, which functions as the heat source. The temperature is monitored using a thermometer, and the temperature is kept constant within 5 degrees. Only once the solution reaches the desired temperature is the substrate placed in the beaker. Various experiments are tested changing variables such as time, temperature, concentration and substrate, keeping the temperature in the range of 55-85 °C and varying the time between 1-3 hours. Table 2.2 shows each experiment's parameters.

Table 2.2 Parameters for Wet Chemistry Experiments

Sample	Substrate	Solution Concentration (M)	Temperature (ºC)	Deposition Time (minutes)
001	Au	0.02M	65º C	180 min.
002	Au	0.02M	65º C	120 min.
006	Au	0.02M	80º C	120 min.
007	Au	0.02M	75º C	120 min
009	Al	0.02M	75º C	75 min.
010	Al	0.02M	65º C	75 min.
011	Al	0.1M	65º C	75 min.
012	Al	0.1M	65º C	120 min.
013	Al	0.1M	80º C	75 min.
014	Ag	0.02M	55º C	75 min
015	Ag	0.02M	65º C	75 min
016	Ag	0.02M	75º C	75 min
017	Ag	0.02M	75º C	75 min

After each experiment, the substrate is rinsed in DI water from plastic container and air dried at room temperature.

2.3 Analysis

2.3.1 Scanning Electron Microscopy

A JSM-7400F Field Emission Scanning Electron Microscope (FESEM) set with an accelerating voltage between 1.0 and 3.0 kV is used to view images of prepared samples. The 7400F is a high resolution SEM that uses a field emission gun as the electron source. At 1kV, it has a resolution of 1.5nm. The detection mode is usually set to lower secondary electron image (LEI) and the magnification ranges from 5,000X- 15,000X. The secondary electron image gives the best resolution because secondary electrons are excited by the electrons incident on the specimen, while the diffusion of incident electrons have little influence on the image. The working distance, distance between underside of the object lens and specimen surface is usually set at 7mm.

2.3.2 Symmetric X-Ray Diffraction

The structural analysis used was x-ray diffraction. A high energy source produces an x-ray beam; the sample placed in the beam's path diffracts the x-rays in a pattern unique to the lattice structure of the crystal. Also, the diffracted pattern intensity is counted at the specific angles with a rotating detector. The

Bragg equation, $\lambda = 2d \sin \theta$, represents the mathematical relationships for an analysis; where d is the spacing between each lattice, θ is the angle of diffraction and λ is the wavelength of the x-ray beam. A Philips/Norelco 1316/92, with a Cu tube for generation of x-rays at 8.04 keV, is used to perform a broad scan of 2θ between 30º and 80º in increments of 0.02°. A fine scan between 32º and 35º, with increments of 0.01°, is also performed. This data is used to confirm that ZnO is present on the surface.

CHAPTER 3

RESULTS AND DISCUSSION

3.1 Electrodeposition

Through electrochemical experiments, ZnO nucleation and growth appears promising, although difficult. Shown below are SEM images of a few of the experiments described previously in Table 2.1.

Upon analyzing the SEM images of deposits, the first conclusion that can be made is that ZnO is electrodeposited. Clearly noticeable is the hexagonal shape which ZnO exhibits due to its hexagonal crystal structure. The ZnO platelets that are grown vary in size for each experiment and vary in size within the same sample. However, each electrodeposition results in nucleation and growth of zinc oxide platelets of approximately 1 μm size. The current passed through the solution during the electrodeposition was initially on the order of 0.05 mA and decreased during the course of the deposition, sometimes to below being detectable.

Initially, ZnO was deposited from 0.05 M $ZnCl_2$ solutions. The initial deposits appeared random although a few structures appear to be platelets with hexagonal symmetry, approximately 3μm in diameter, shown in Figure 3.1. The

fact that platelets are growing instead of the small hexagon columns that have been reported in the literature [8] suggests that under these growth conditions, the structures are not growing along the (0001) face but along the ($\underline{1}$010), (10$\underline{1}$0), (0$\underline{1}$10), (01$\underline{1}$0), (1$\underline{1}$00) and ($\underline{1}$100) faces.

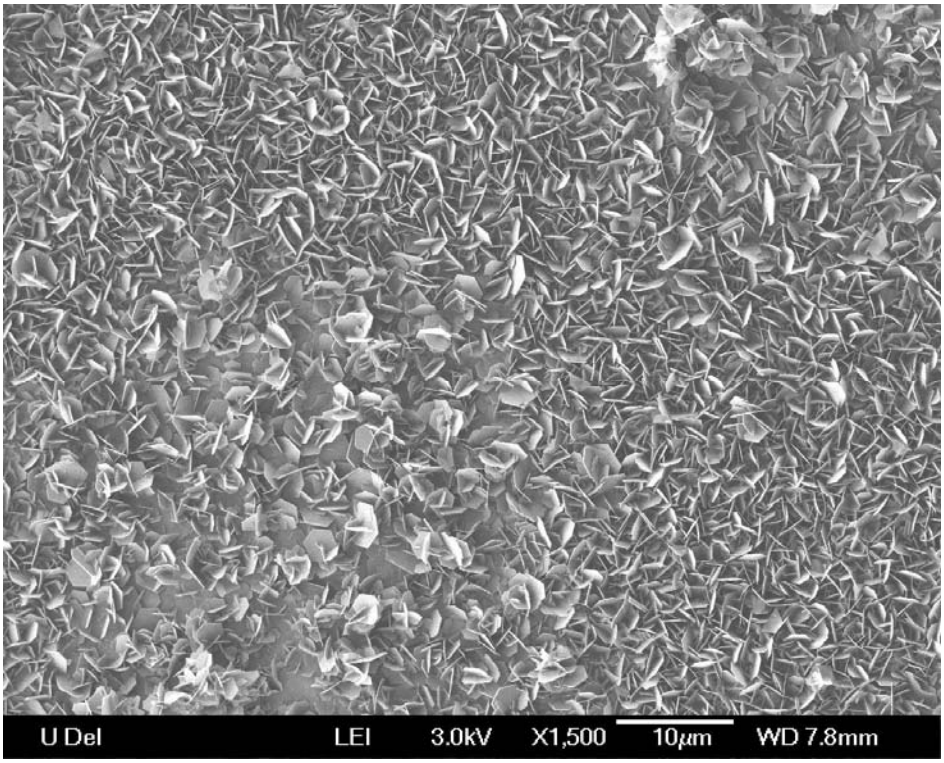

Figure 3.1 Sample 01 has hexagonal ZnO platelets approximately 3000 nm in diameter. Growth conditions were 0.05 M $ZnCl_2$, 67°C, -0.7V SCE, 60 minutes on Au substrate.

To study the effects of growth deposition time, sample 07 was grown under the same conditions as sample 01, but for 45 minutes instead of 60 minutes; Sample 07 also shows 2 μm hexagonal platelets which are slightly distorted. However many platelets appear to lay flat on the surface of the substrate.

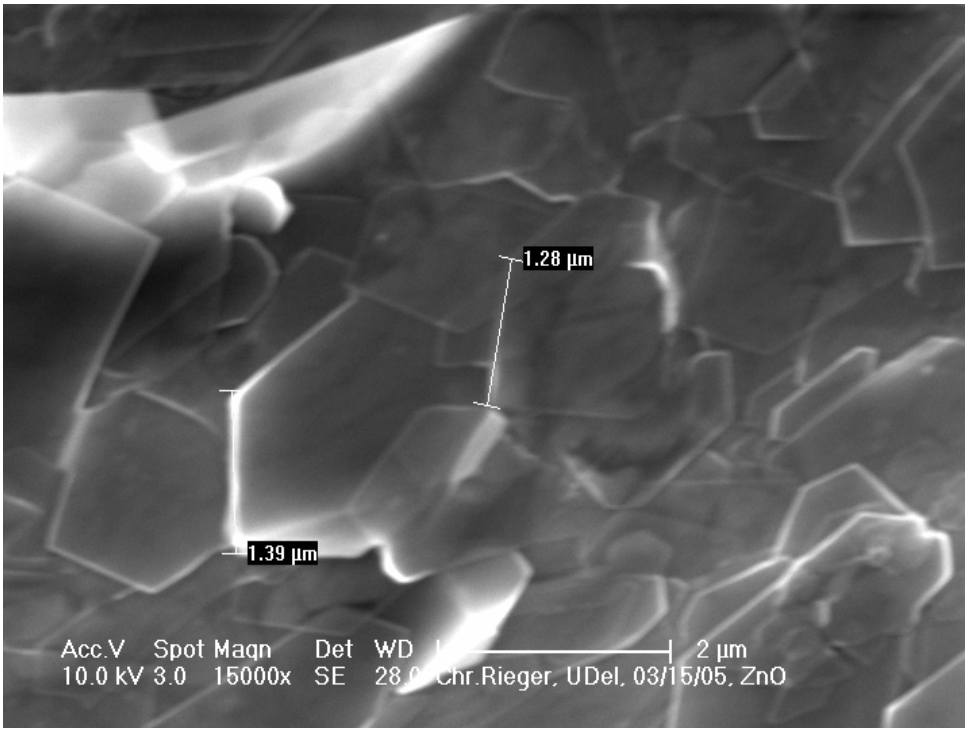

Figure 3.2 Sample 07 has hexagonal ZnO platelets approximately 2000 nm in diameter. Growth conditions were 0.05 M $ZnCl_2$, 67-70°C, -0.7V SCE, and 45 minutes on Au substrate.

Sample 06 was grown under the same conditions as the previous samples (samples 01 and 07), however deposition time is even shorter, 20 minutes. The ZnO platelets are approximately the same size as the platelets in sample 01, about 3μm in diameter. In Figure 3.2 a cross sectional view of sample 06 which shows that randomly grown platelets vary in diameter across the substrate. Furthermore, it is evident that many of the platelets have not nucleated at the surface of the sample but as part of the previously grown platelets. A careful examination of Figures 3.1, 3.2, and 3.3 does not show an obvious change in growth upon changing the growth time by a factor of three.

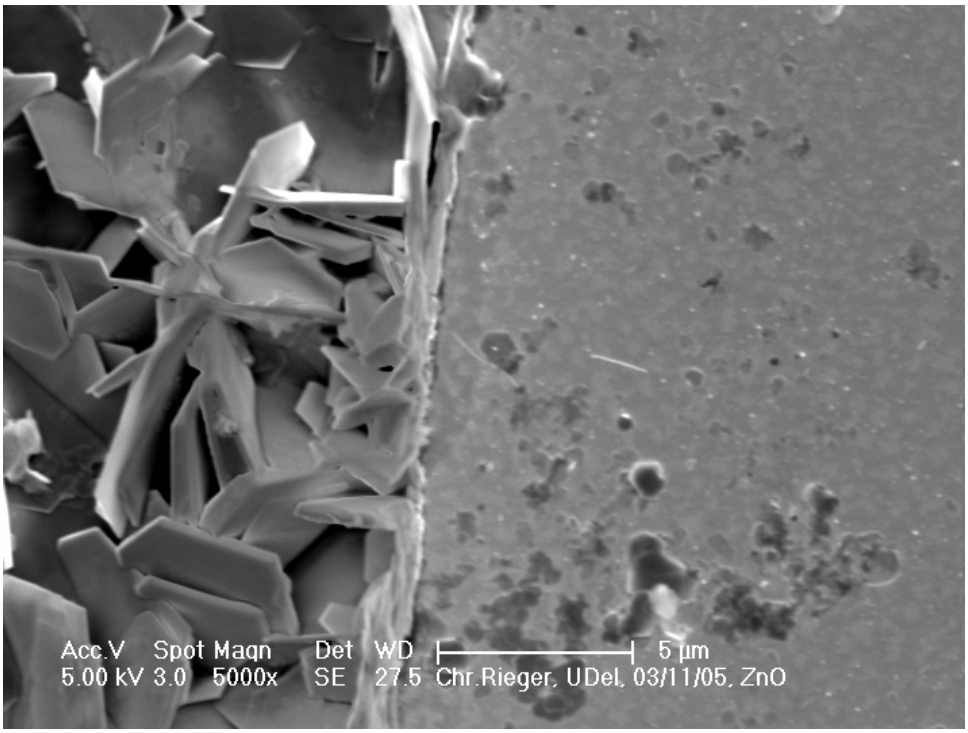

Figure 3.3 Sample 06, in cross section has hexagonal ZnO platelets approximately 3000 nm in diameter Growth conditions were 0.05 M $ZnCl_2$, 67°C, -0.7V SCE, 20 minutes on Au substrate.

Sample 08 was grown under the same conditions as the previous three depositions, except slightly longer than the first experiment, 70 minutes. The platelets again vary in size with slight distortion; most appear to lay flat on surface although some are turned on edge. Thus changing the growth time from 20 to 70 minutes has not radically changed the growth pattern.

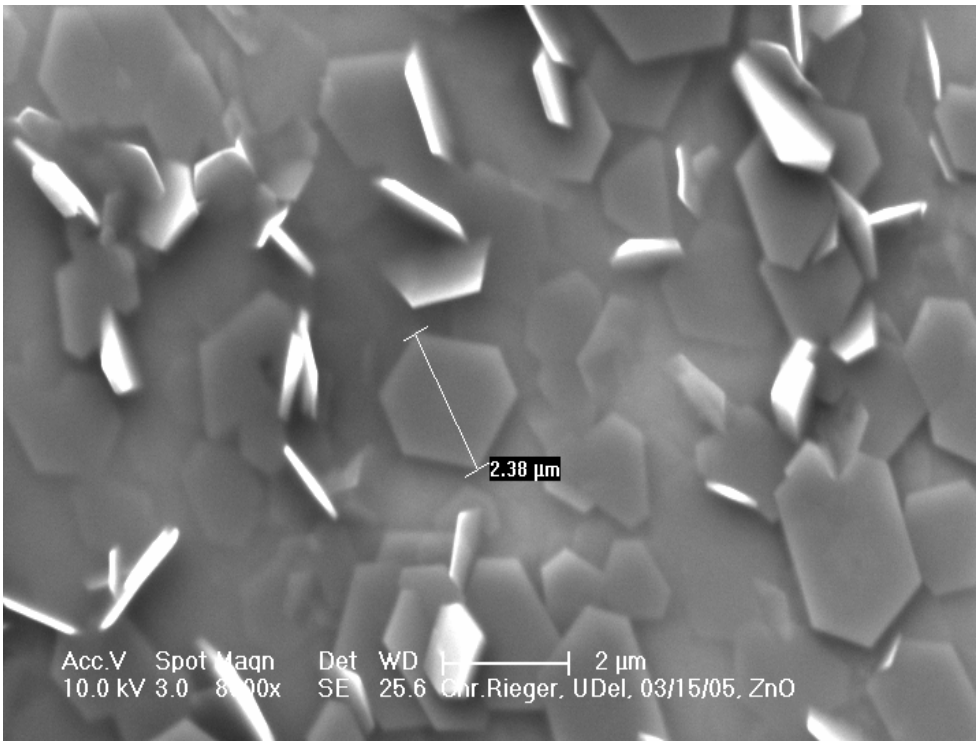

Figure 3.4 Hexagonal ZnO platelets approximately 2400 nm in diameter. Growth conditions were 0.05 M $ZnCl_2$, 67°C, -0.7V SCE, 70 minutes on Au substrate.

To summarize, growth with a potential of -0.7 SCE at 67°C, for a period of 20 to 70 minutes, appears to result in the deposition of platelets with a (0001) orientation. Most of the growth appears to be along the edges of the platelets resulting in very thin platelets. Plan view secondary electron micrographs suggest that the platelets are orientated parallel to the substrate surface. However a cross section view shows that many of the platelets are in fact perpendicular to the surface. Because electric field is likely to be concentrated at the edge of the

platelet during deposition growth is also likely to occur there. Apparently the relative roughness of the edges causes deposition to occur preferentially there, rather than on the flat (0001) plane, resulting in the growth pattern observed here.

The growth conditions of sample 09 were similar to the previous samples, except the potential was increased to -0.6V SCE. A cross sectional view of Sample 09 (Figure 3.5) shows the ZnO platelets, but also demonstrates the fact that columns are still not present. A few of the hexagonal platelets are noticeable, although the increase in potential seems to cause some distortion of the sample.

If the growth observed is due to field concentration at the edges and growth on the relatively rougher ($\underline{1}010$), ($10\underline{1}0$), ($0\underline{1}10$), ($01\underline{1}0$), ($1\underline{1}00$) and ($\underline{1}100$) faces, the fact that the same growth mode is not observed is not unexpected.

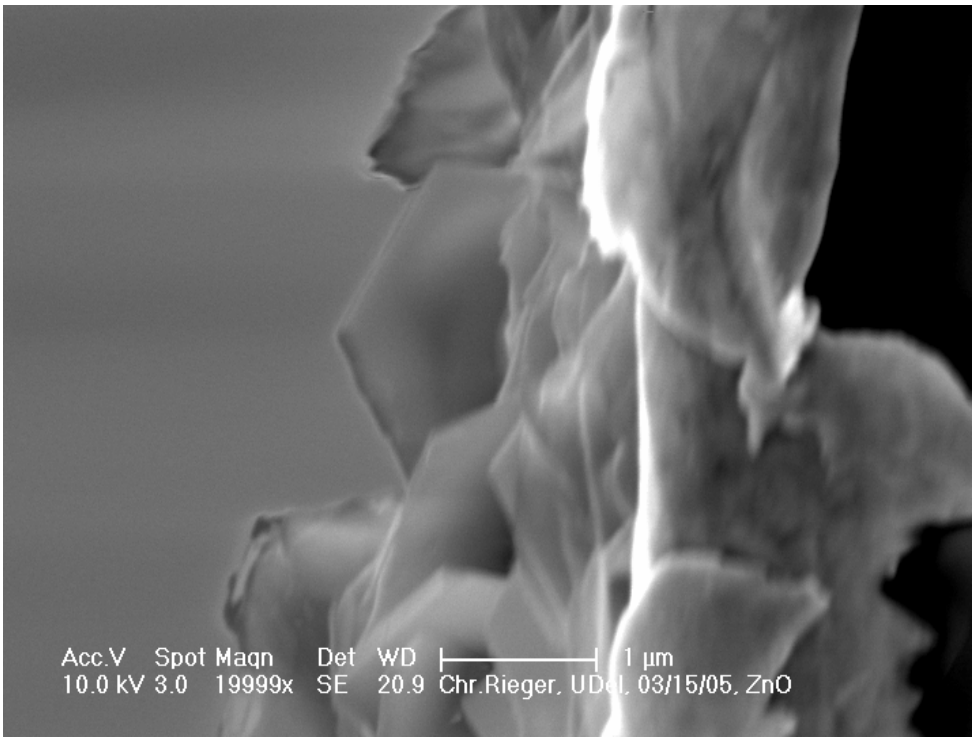

Figure 3.5 Cross sectional view of sample. Growth conditions were 0.05M $ZnCl_2$, 67-70º C, -0.6V SCE, and 20 minutes on Au substrate.

Because varying the potential did not produce results resembling the nanorod structure desired, the concentration of $ZnCl_2$ was reduced. Sample 10 shows flatly grown platelets varying in size having an overlapping growth; these platelets are roughly the same size as the structures in previous samples using a greater $ZnCl_2$ concentration. Upon changing the concentration of $ZnCl_2$ in the solution to .025 M, the platelets still appear to lay flat on top of the substrate, as seen in the plan view micrographs shown in Figures 3.1, 3.2 and 3.4 above. While

all of the platelets still have an approximately hexagonal shape, the sides of the hexagon are not even. Because of the decreased concentration, and the decreased resistivity of the solution, the fields will be even more concentrated at the edges, and thus most of the growth will be even more restricted to the edges.

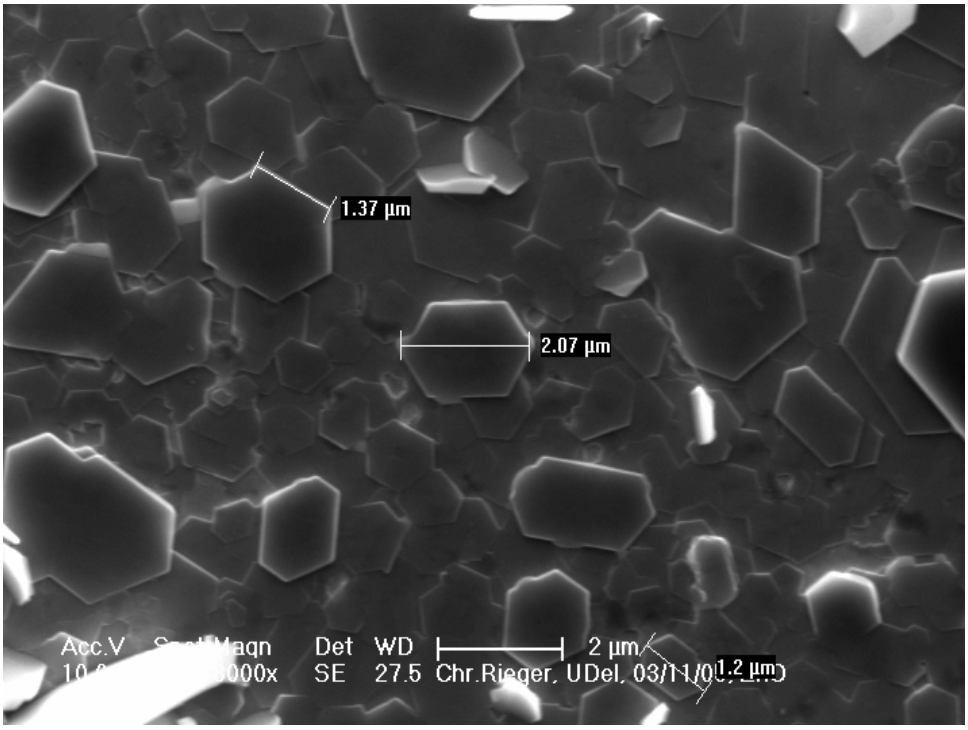

Figure 3.6 Depicted are actual dimensions of ZnO platelets ranging from 1320nm-2070nm in diameter. Growth conditions were 0.025M $ZnCl_2$, 67-70º C, -0.7V SCE for 20 minutes on Au substrate.

Sample 11, grown under the same conditions as sample 10, except for an increase in growth time to 45 minutes, shows clumps of ZnO platelets on some areas of the surface (Figure 3.7). In those areas there are some very large platelets, with some smaller ones nucleated on the large platelets. Note also that more platelets seem to have a random orientation on the surface.

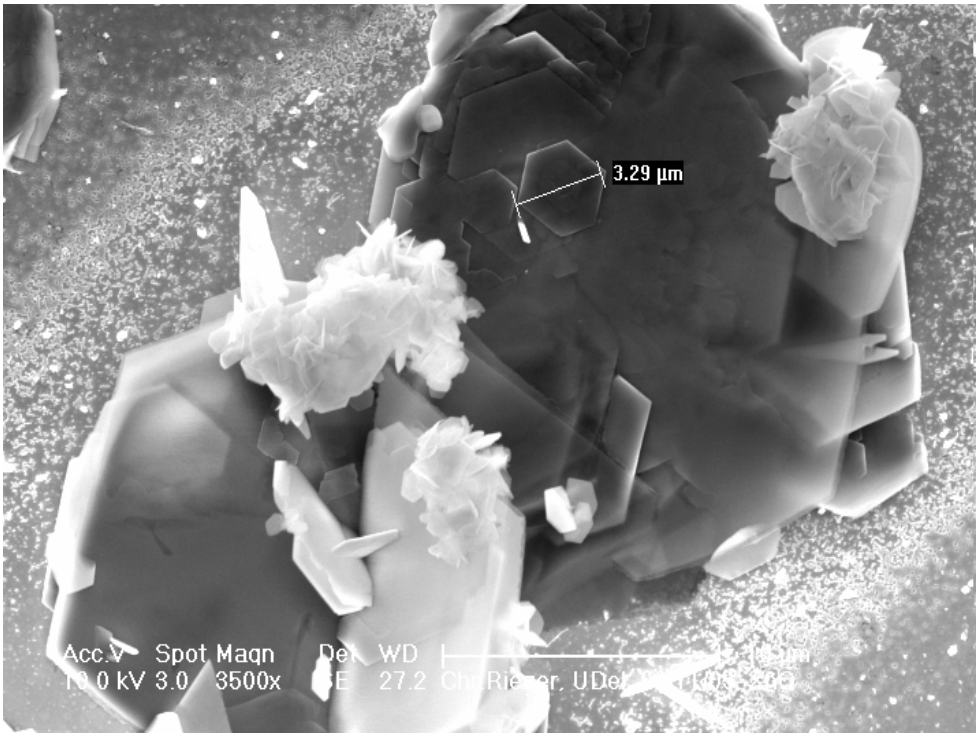

Figure 3.7 ZnO platelets vary in diameter. Growth conditions were 0.025M $ZnCl_2$, 67-70º C, -0.7V SCE for 45 minutes on Au substrate.

Sample 12, grown with potential of -0.6 V SCE instead of -0.7 V shows larger clumps of ZnO and a few that lie flat on the surface. (Figure 3.8) The ZnO platelets are distorted, similar to the results from increasing the potential to -0.6V SCE that is shown in Figure 3.5. Apparently this potential is insufficient to cause enough electric field at the platelet edges to lead to uniform platelet growth.

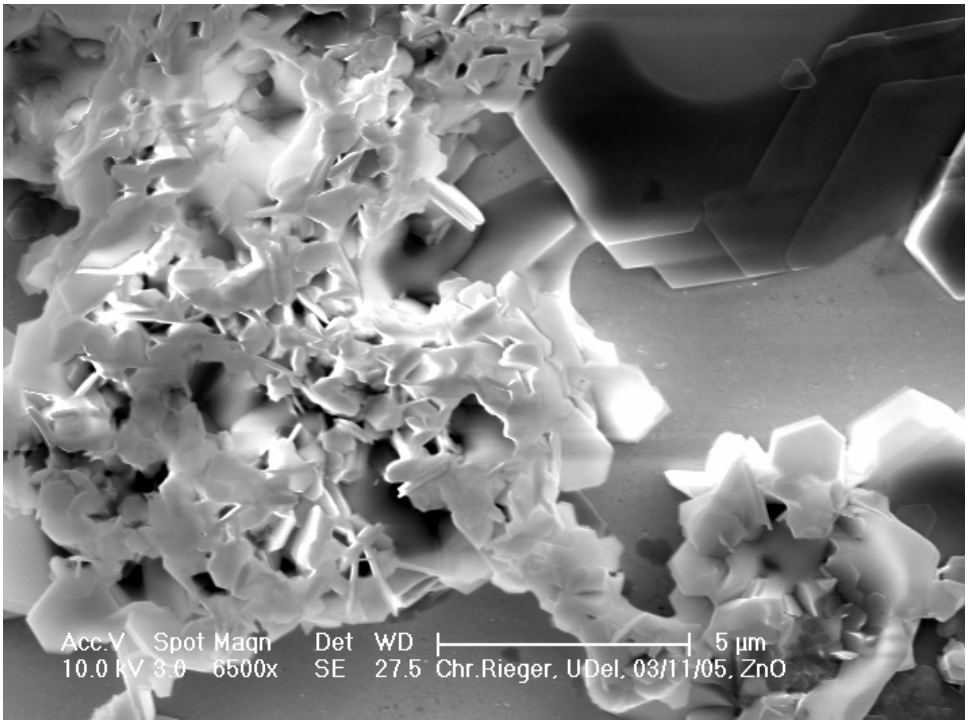

Figure 3.8 ZnO platelets are clustered together. Growth conditions were 0.025M $ZnCl_2$, 67-70º C, -0.6V SCE for 20 minutes on Au substrate.

Decreasing the $ZnCl_2$ concentration by 50% also does not result in the desired nanorod structure (see Figure 3.9). However, the using the lesser concentration some of the platelets on the substrates actually have the (0001) orientation.

The concentration of $ZnCl_2$ was further reduced to .02M (Figures 3.9, 3.10 and 3.11). Figures 3.9 and 3.11 show platelets larger in size than those from the previous experiments; they are about 10 μm in diameter and randomly oriented. This is consistent with the growth mechanism at of the field concentrations at the corners of the platelets and growth preferentially occurring on the non (0001) face. Decreasing the concentration of the ions increases the resistance of the solution which further concentrates the electric field on the corners of the platelets.

Sample 14 has larger platelets approximately 3μm in diameter, while there also appears to be smaller ZnO crystals roughly 200nm in diameter.

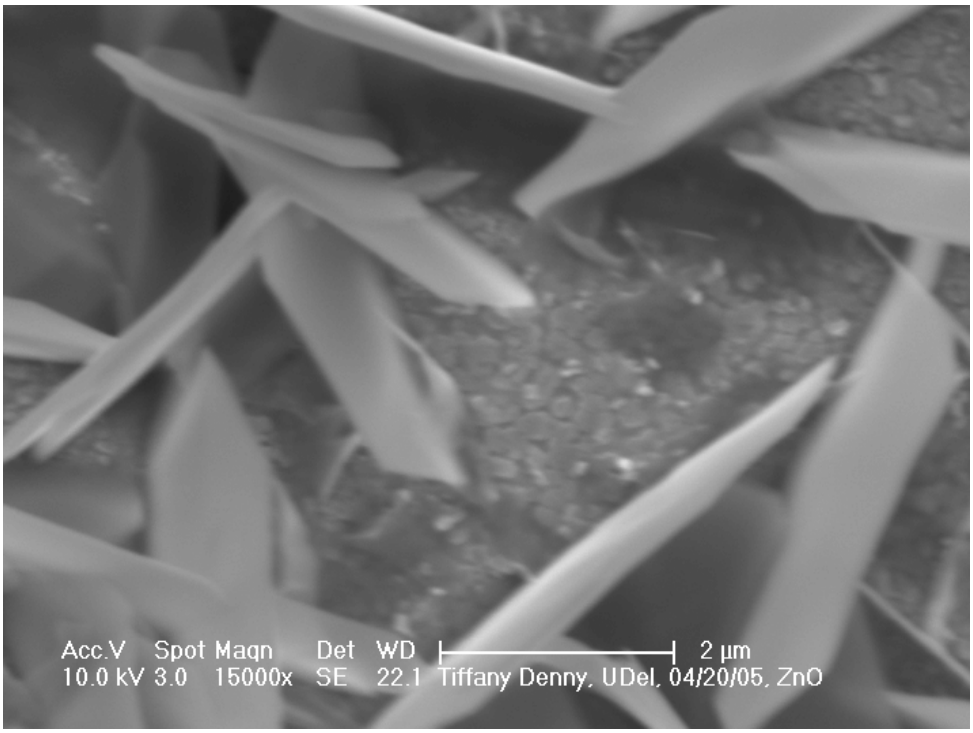

Figure 3.9 ZnO platelets, grown randomly, are approximately 3µm in diameter. Growth conditions were 0.02M $ZnCl_2$, 67-70º C, -0.7V SCE for 20 minutes.

For the next electrodeposition experiment, what happens after just a few minutes of growth is examined. The deposition time was decreased to 5 minutes. The hexagonal shape is vaguely visible on this sample; the diameter is approximately 300nm, which is consistent with a majority of the previous experiments. The sample shown in Figure 3.10 shows ZnO in a very different conformation, and although the hexagonal shape is not as defined as the other images, they are present. This sample is somewhat promising in that the structures

appear to be incipient columns, which were sought in these experiments. This experiment suggests that there is an incubation time before nucleation occurs. Once nucleation occurs, growth follows.

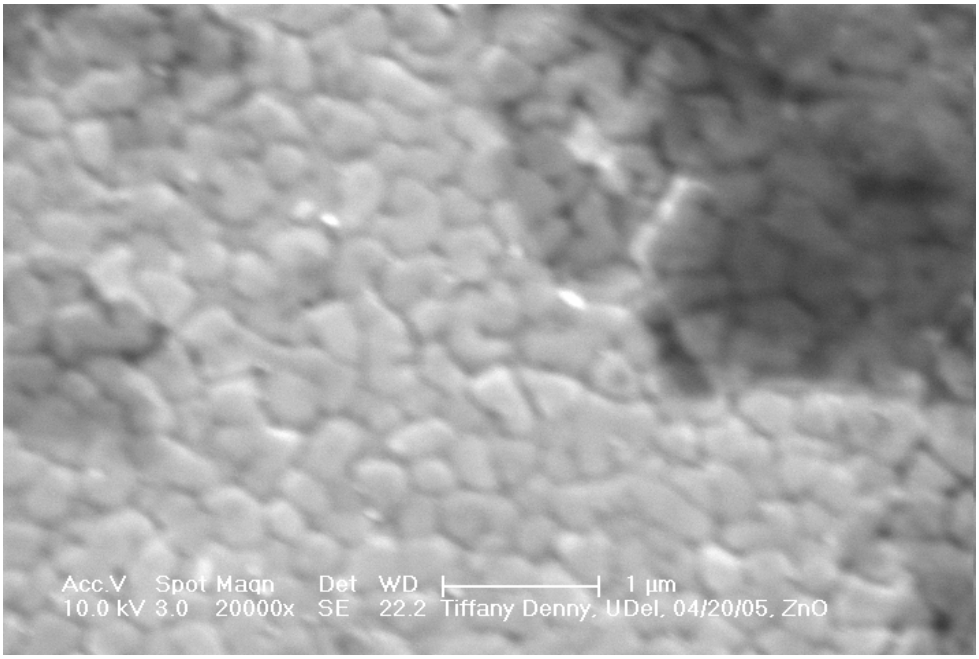

Figure 3.10 The beginning growth of ZnO nanostructures. Growth conditions were 0.02M $ZnCl_2$, 70º C, -0.7V SCE for 5 minutes on Au substrate.

Growth conditions are consistent with the previous two samples except that the potential is decreased to -0.8V Sample 18 displays larger hexagonal platelets approximately 13µm in diameter; however half of each platelet appears to nucleate

into the surface of the substrate (Figure 3.11). Here, the larger platelets result from greater fields leading to an increased growth along the edges.

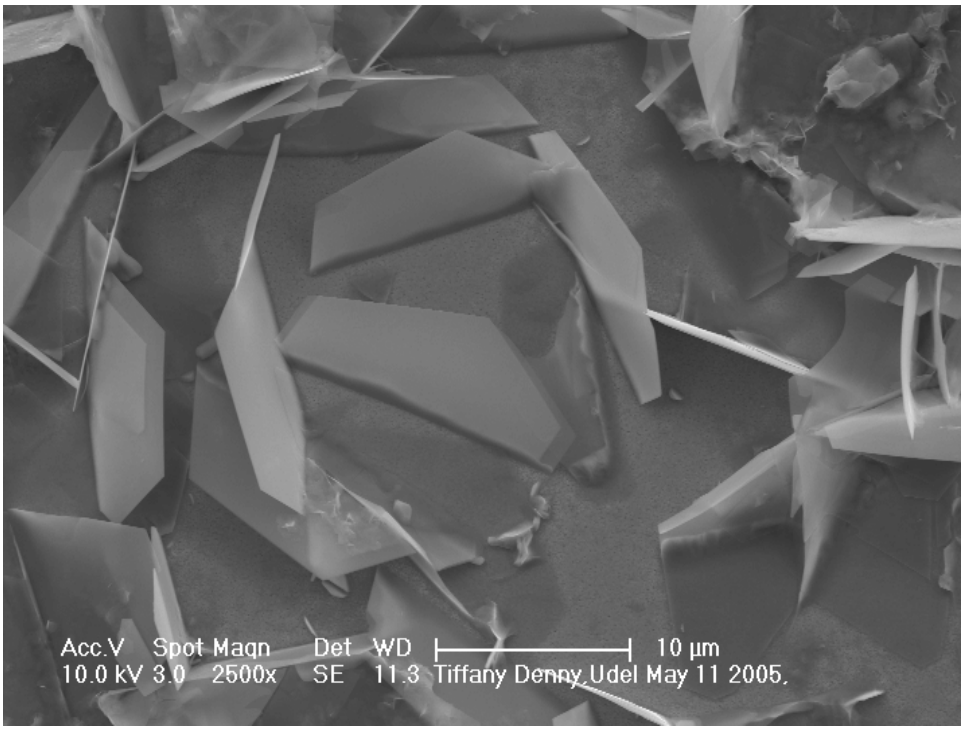

Figure 3.11 ZnO platelets, 13 µm in diameter, nucleate into the surface of the substrate. Growth condition were 0.02M $ZnCl_2$, 67º C, -0.8V SCE for 20 minutes on Au substrate.

It is not evident as of yet if these platelets or nano structures will have any importance for electronics devices. However, for the future goals based on the progression of this research, the platelets and random structure are not the optimal

structures that are needed. Perhaps future experiments will examine higher concentrations of $ZnCl_2$ and larger potentials may solve of the concerns brought forth, so that the growth dynamic can be changed. Thus, another deposition method was sought.

3.2 Wet Chemistry

Experimenting with an alternative wet chemistry method became essential when expected results were not obtained using electrodeposition. The results from wet chemistry are an improvement, and promising for future work. The first few experiments are performed on single crystal Au (Figures 3.12-3.15). Rod-like hexagonal ZnO structures are present; although, they are clumped together in groups and they are not perpendicular to the surface of the substrate.

Across several sections of the surface of sample 001, shown in Figure 3.12, are ZnO rod-like structures about 500nm in diameter nucleated and grown into each other, however the hexagonal shape is still noticeable. Growth in the (0001) direction is evident.

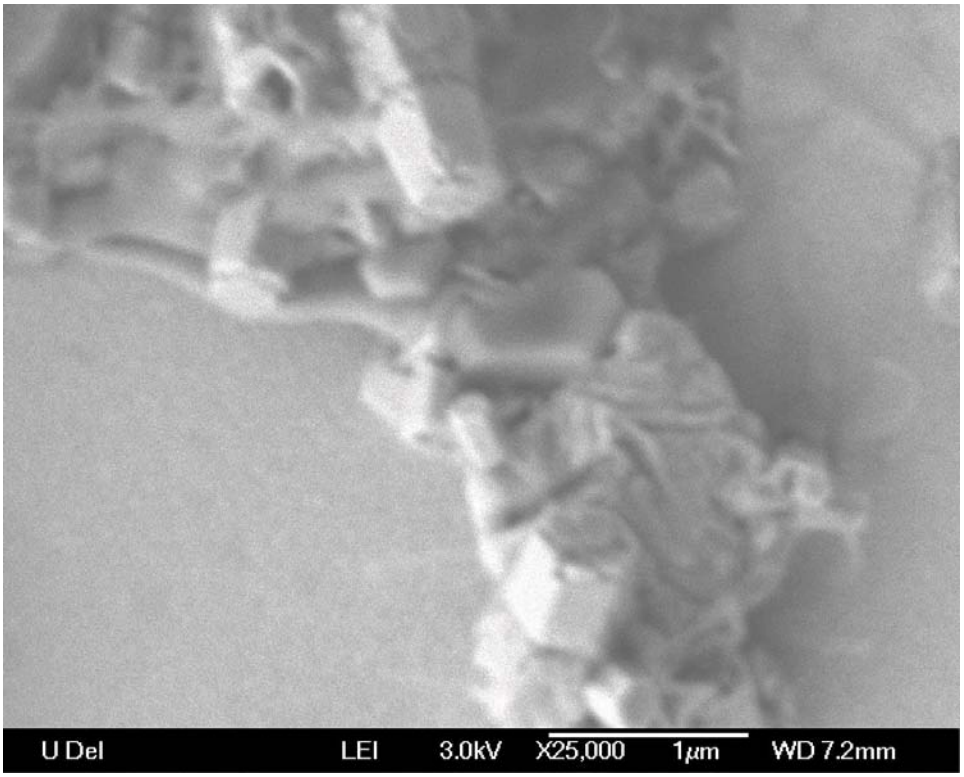

Figure 3.12 ZnO cluster of nanorods. Growth conditions were equimolar 0.02M concentration, 65ºC for 120 minutes on Au substrate.

The growth conditions in Figure 3.13 were the same as sample 001, except there was an increase in deposition time from 120 to 180 minutes. Hexagonal shaped rods, ranging from 200-500nm in diameter are displayed, but they are packed together and not perpendicular to the surface of the substrate. The micrographs make it unclear where the columns have nucleated. The size of the

columns has not changed, but the number appears to have increased, suggesting that rods nucleate, grow quickly, and then cease.

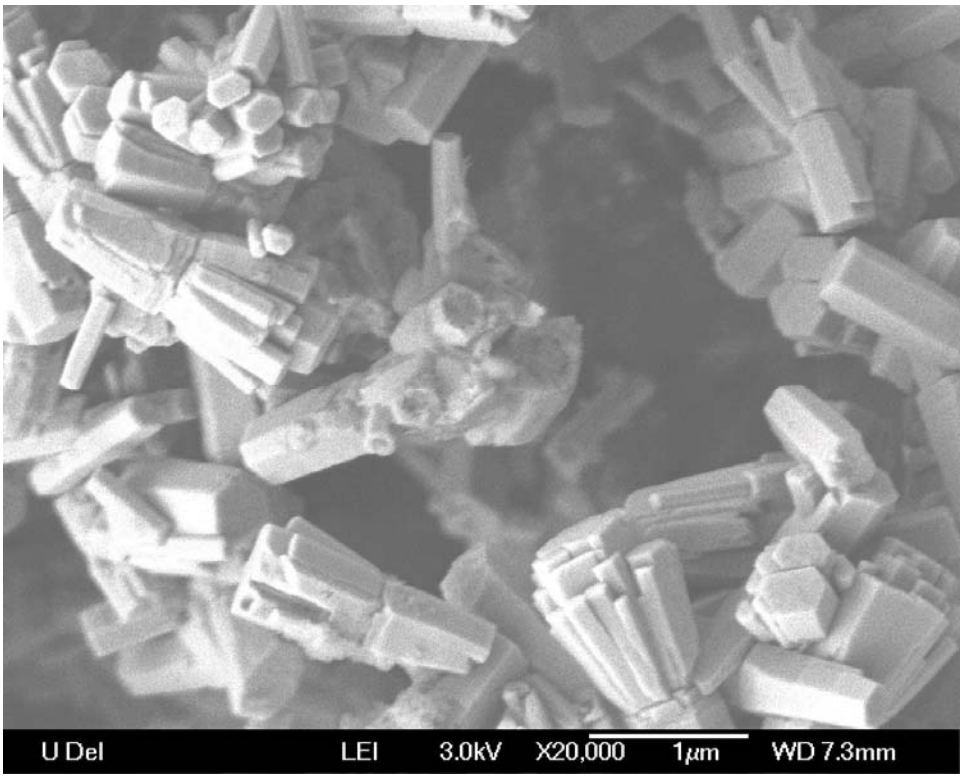

Figure 3.13 ZnO cluster of nanorods, about 300nm in diameter. Growth conditions were 0.02M solution, 65º C for 180 minutes on Au substrate.

The temperature was increased to 80º C and above during the 120 minutes of deposition time. Sample 006 shows no rod-like structures like the previous two samples. Because the solubility of Zn^{2+} ions increases at greater temperatures, this may increase the dissolution of the columns, resulting in disorganized growth.

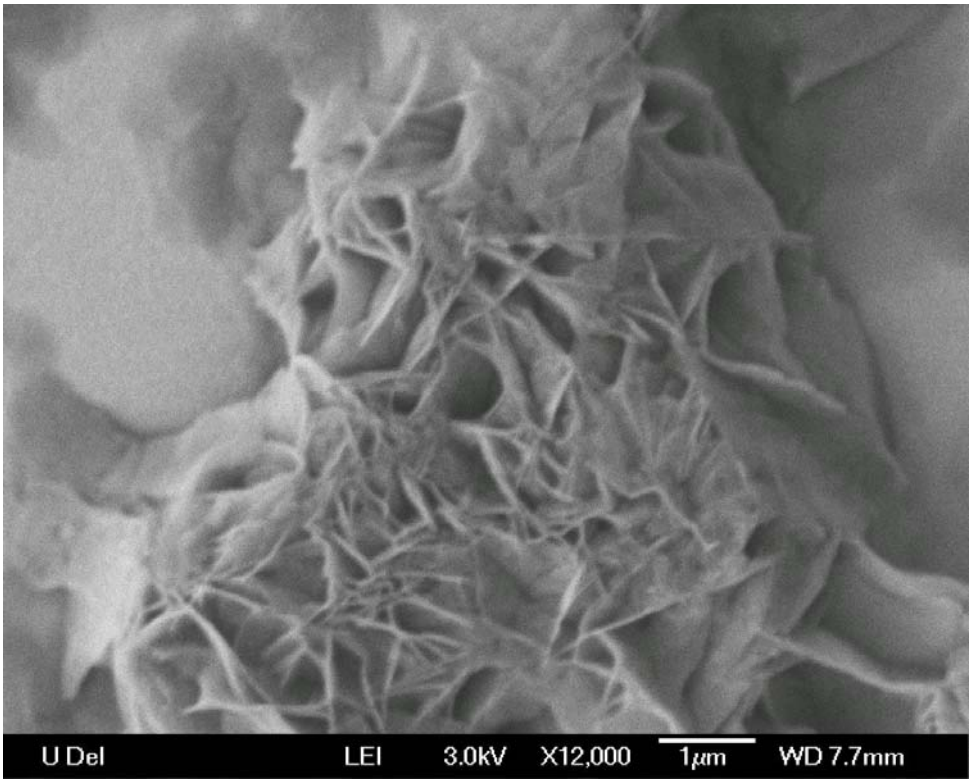

Figure 3.14 ZnO random distorted growth. Growth conditions were 0.02M, >80º C for 120 minutes on Au substrate.

The temperature setting for the following experiment was decreased somewhat to 75º C, and the ZnO rods become visible, ranging in sizes from 2000-4000nm in diameter. However, some of the structures appear to be distorted.

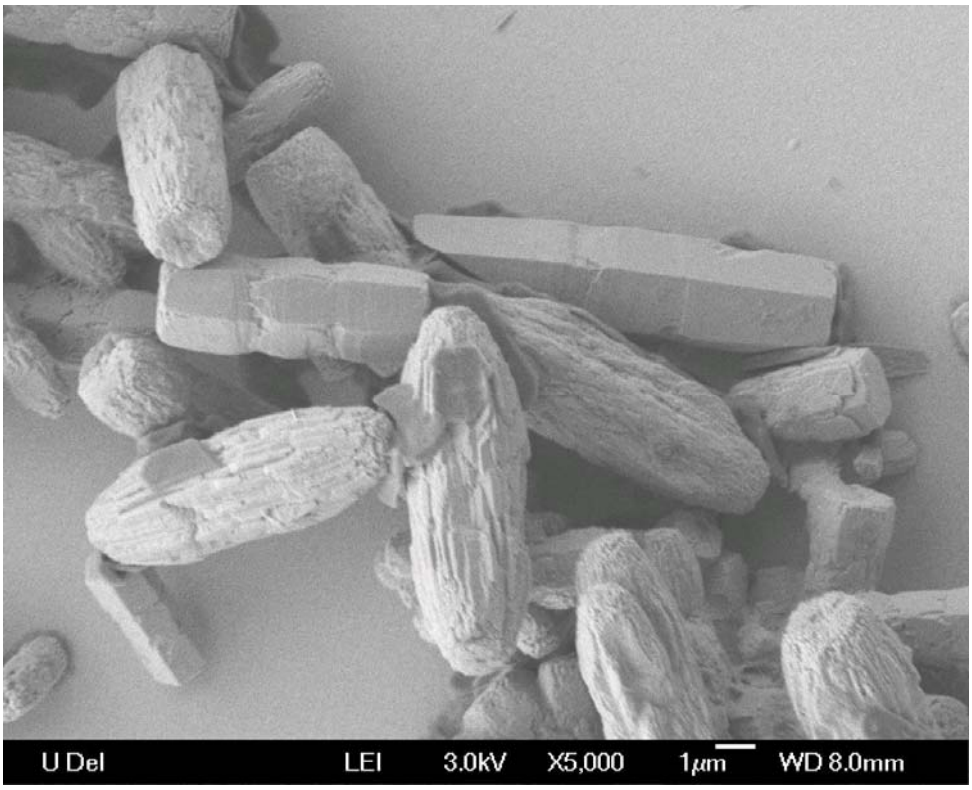

Figure 3.15 ZnO rods shown with slight distortion. Growth conditions were 0.02M, 75º C for 120 minutes on Au substrate.

The next set of experiments was done on an Al substrate (Figures 3.16-3.20). The first couple of trials were completed using 0.02M solution. The hexagonal nanorod structures are not as clumped together as before, but they are not facing the desired direction. The concentration is then changed to 0.1M, five times the concentration used previously. Figure 3.18 depicts ZnO nanoparticles mostly perpendicular to the surface and approximately consistent in size throughout

the surface. Some overlapping occurs. In Figure 3.19, where the deposition time is twice as long, there are hexagonal platelets instead of the rods expected. Figure 3.20 shows random growth, attributed to the high deposition temperature which was > 80º C.

The Al substrate also allows for ZnO microrod growth and nucleation. Hexagonal shape rods still grow into each, are not perpendicular to surface, and are larger than 1μm in diameter. The ZnO columns grown on Al have a larger diameter than those grown on Au.

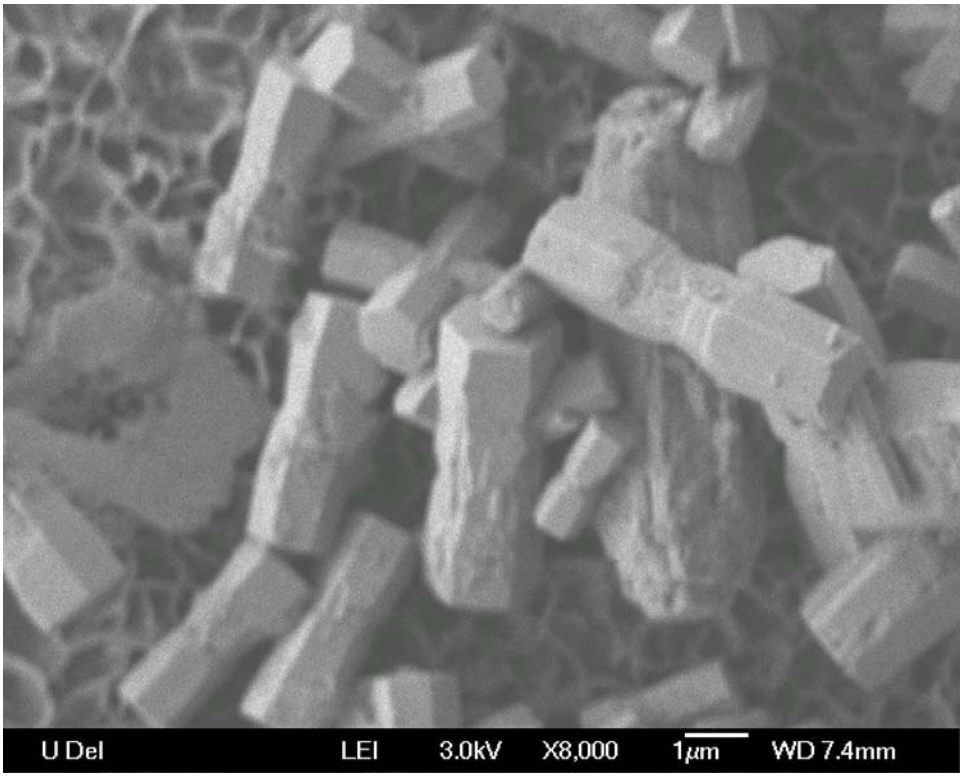

Figure 3.16 ZnO rods approximately 1.5 μm in diameter. Growth conditions were 0.02M, 75º C for 75 minutes on Al substrate.

The growth conditions are the same as the previous experiment, except the temperature was decreased to 65º C. Sample 010 shows a similar variation in size of the hexagonal structures, as seen for the 75º C growth; some are approximately 1μm in diameter and other are about 500nm.

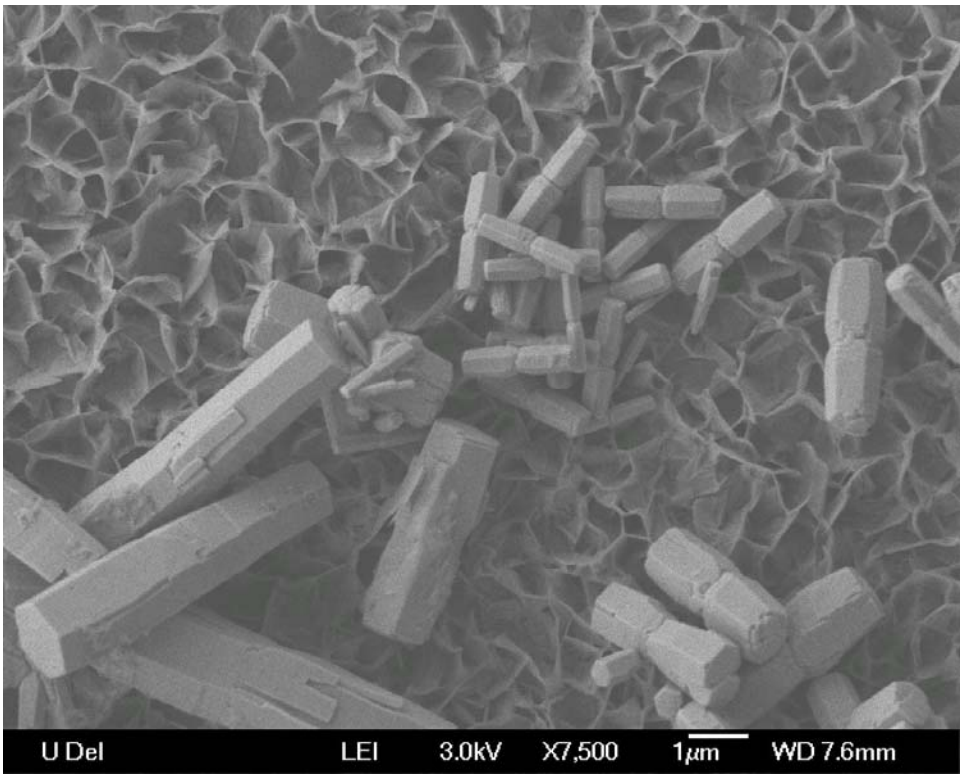

Figure 3.17 ZnO rods ranging from 500nm – 1 μm in diameter. Growth conditions were 0.02M, 75º C for 65 minutes on Al substrate.

The concentration was increased to 0.1M, 5 times what has been previously used. The platelets, with a diameter of 500nm, are even sided, unlike some of the ones grown using electrodeposition and most have the (0001) plane parallel to the surface. They also appear to be somewhat shorter.

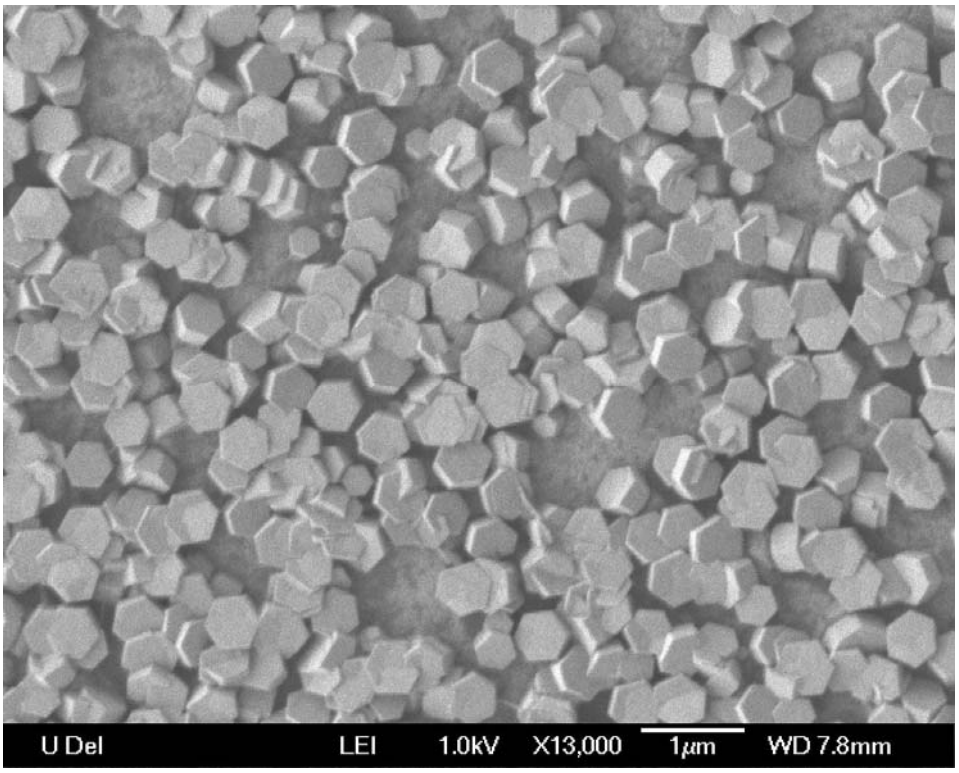

Figure 3.18 ZnO platelets, 500nm in diameter. Growth conditions were 0.1M, 65º C for 75 minutes.

The same growth conditions as above were used, however instead the deposition time is increased to 120 minutes. Once again, even sided platelets are observed and are roughly 500nm in diameter, same as the platelets in the previous deposition.

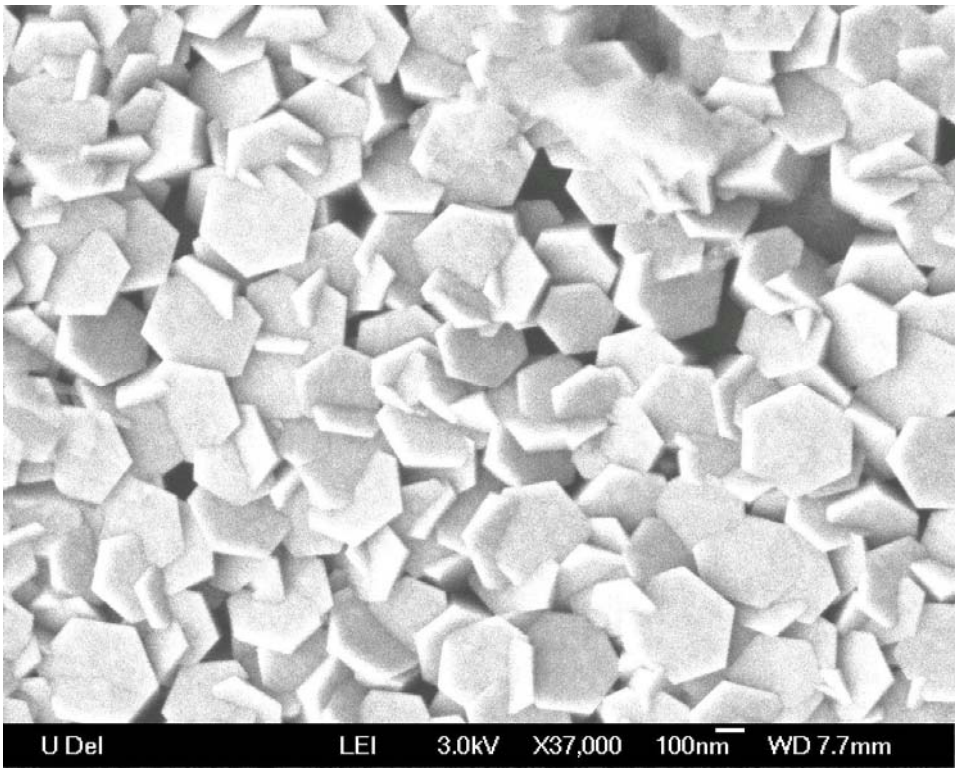

Figure 3.19 ZnO platelet structures 500nm in diameter. Growth conditions were 0.02M, 65º C for 120 minutes on Al substrate.

The time difference in the previous two experiments did not make a difference in the type of structures that were grown; therefore the temperature is increased above 80º C. ZnO rods are visible, but the heat has also seemed to cause a bit more nucleation and distortion in growth, again presumably because of the increase solubility of Zn^{2+}.

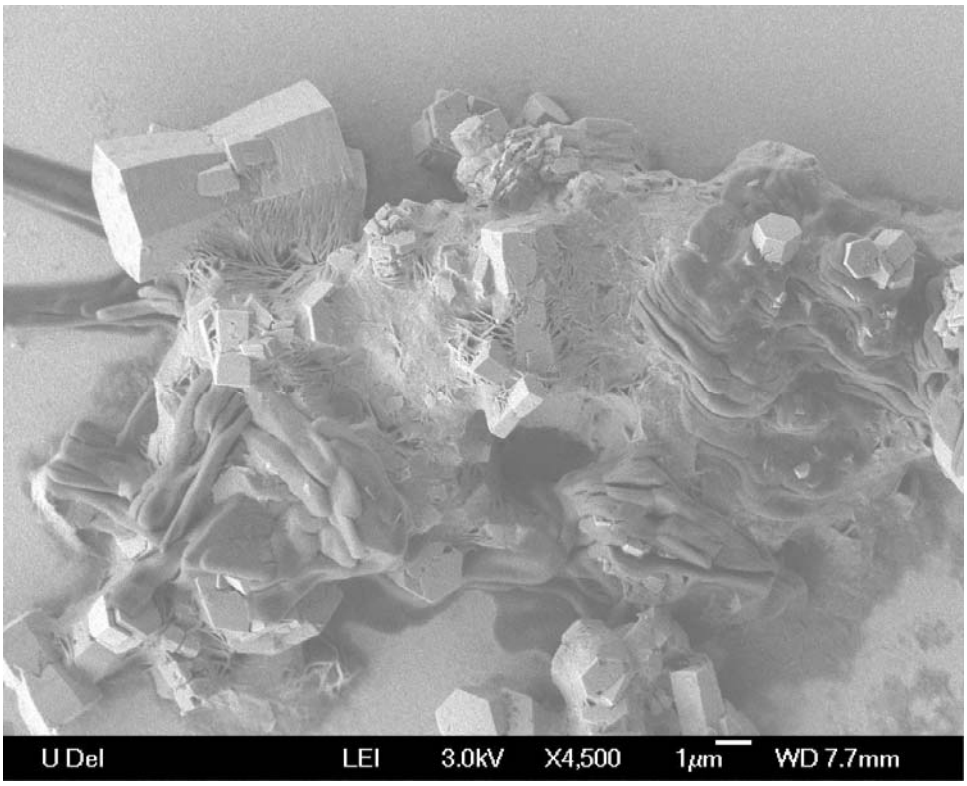

Figure 3.20 A few ZnO rods are visible, but there is a lot of nucleation and growth. Growth conditions were 0.02M, > 80º C for 75 minutes on Al substrate.

The wet chemistry performed on the Al substrate produce ZnO nanorods. For the lesser concentration of 0.02M, the nanorods were not facing the perpendicular direction, but they were growing along the (0001) plane even when the temperature and time was varied. The higher concentration of 0.1M resulted only in platelets, which however were mostly facing perpendicular to the surface. A temperature greater than 80º C seems to results in random growth across several areas of the substrates surface.

Finally, a silver substrate was used for the wet chemistry experiments; the concentration of the solution was 0.02M. The Ag substrate reveals the beginning of some promising results. In Figure 3.21, the SEM image depicts the nanorods perpendicular to the substrate's surface, approximately 100nm in diameter. Although some appear to be slightly bent, it may be still possible to make an electrical contact. The rods are only visible on certain regions of the Ag. The best results are given on the silver substrate this far, more specifically Figures 3.23 and 3.24, which has an array of nanorods.

Some areas of the surface, for the sample grown on Ag at 55º C, have ZnO nanorods approximately 100nm-200nm in diameter and less than 1μm in length. The nanorods are growing perpendicular to the surface, facing the (0001) plane; some are slightly bent. Both the temperature and substrate have been changed in this experiment.

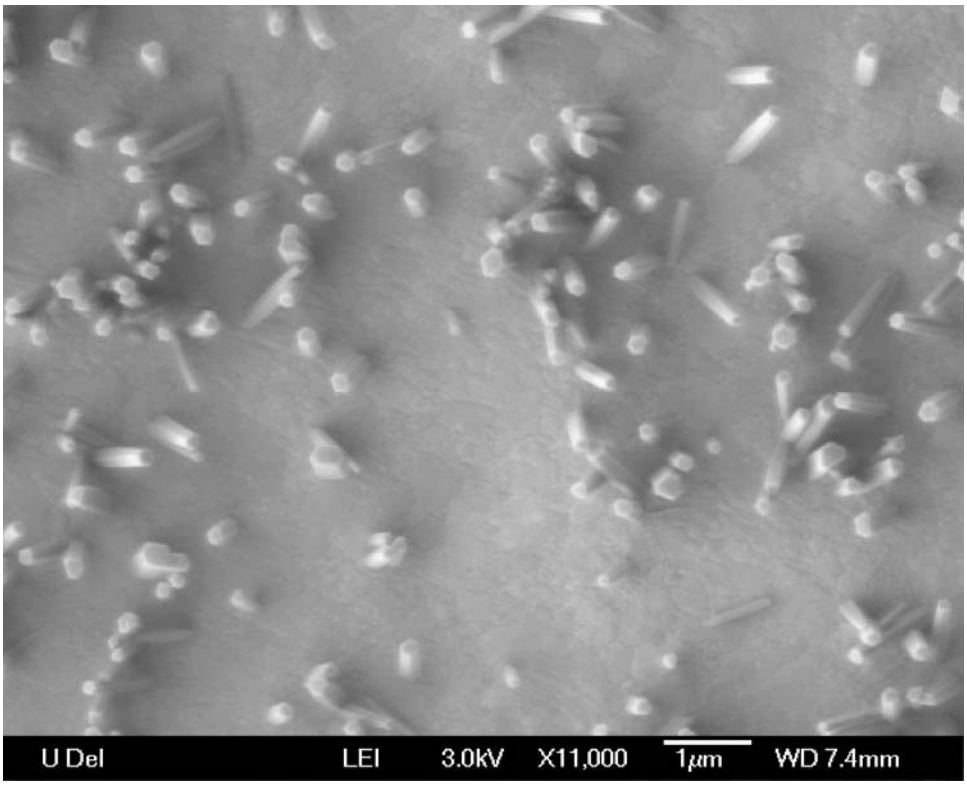

Figure 3.21 ZnO nanorods, about 100-200 nm, are growing along the (0001) plane outward from the surface. Growth conditions were 0.02M, 55º C and 75 minutes on Ag substrate.

The concentration was kept at 0.02M for 75 minutes, but temperature is increased to 65º C. The smaller structures appear to be nanorods; however also growing are the larger rods that nucleate together, which were seen in the first few wet chemistry depositions.

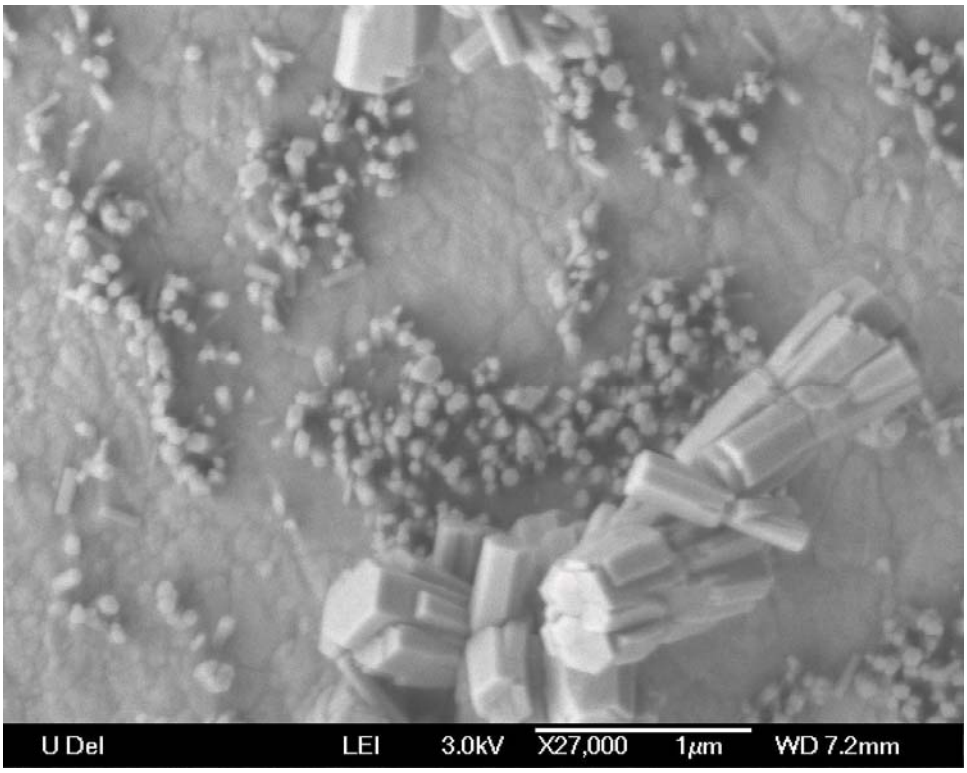

Figure 3.22 ZnO nanorods, approximately 100nm in diameter, grow parallel to the surface. Larger ZnO rods nucleate together. Growth conditions were 0.02M, 65º C for 75 minutes on Ag substrate.

The following deposition involved a temperature increase; ZnO rods are 200nm in width and growing in the optimal direction. In addition, the larger columns that have fallen over are not evident.

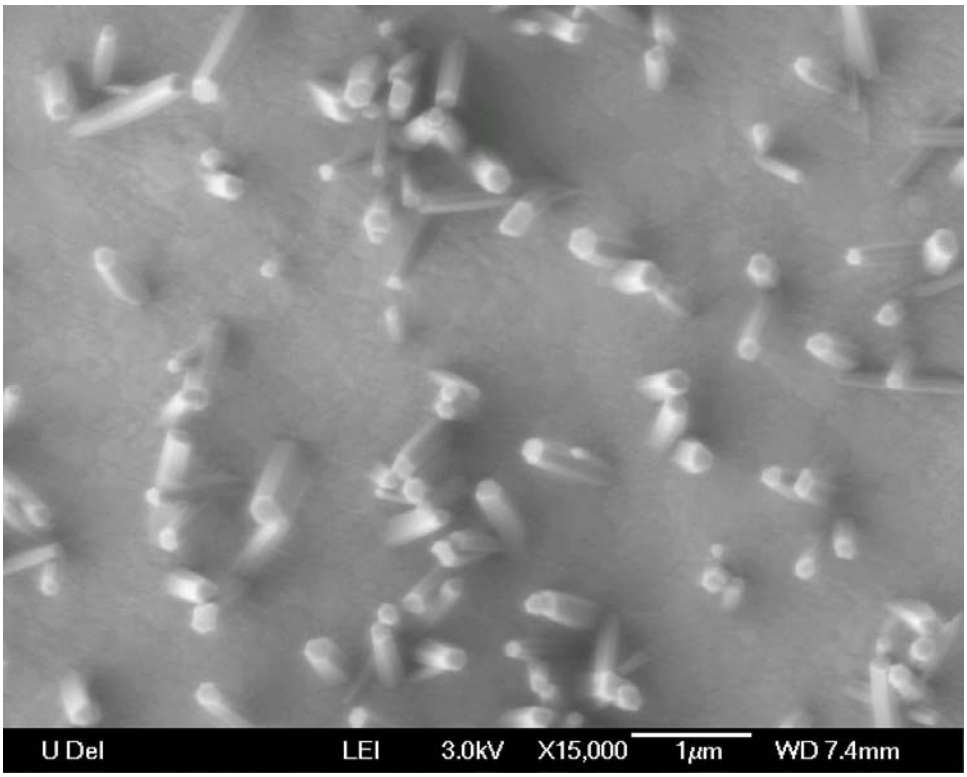

Figure 3.23 ZnO nanorods, 200nm in diameter, grow along the (0001) plane. Growth conditions were 0.02M, 75º C for 75 minutes on Ag substrate.

The conditions for the sample shown in Figure 3.23 were repeated to see if same results will be produced. And, the growth conditions used for this deposition proved to give the best results. The ZnO nanorods are 200nm in width and less than 1μm in length. However, the density of columns appears to be greater.

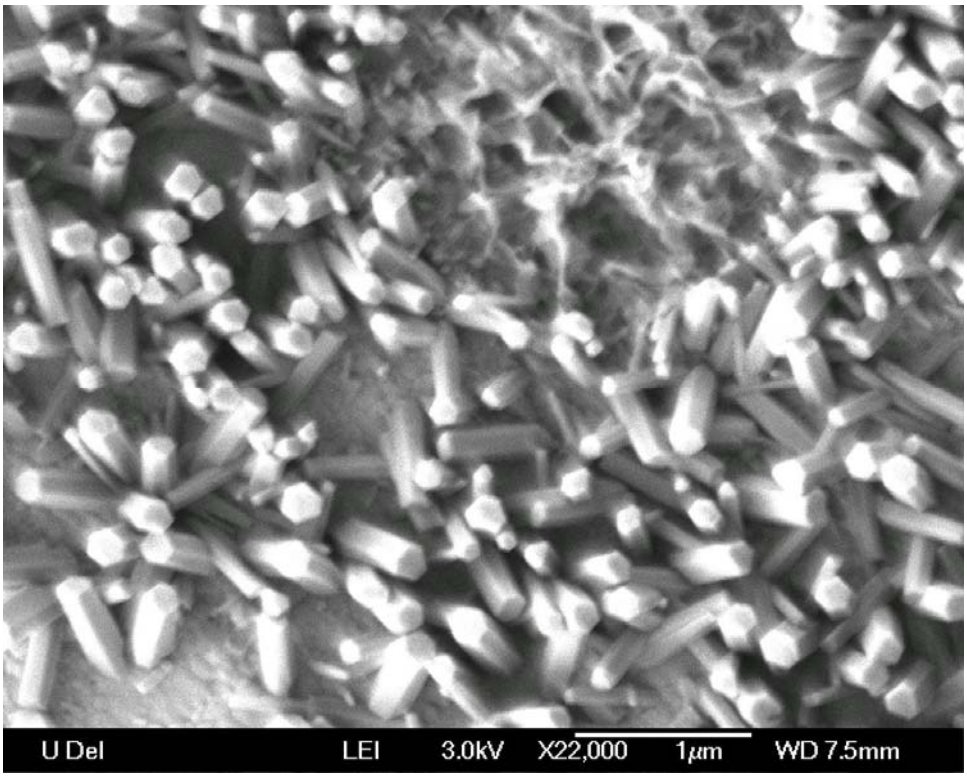

Figure 3.24 ZnO nanorods, 200nm in diameter, grow along the (0001) plane. Growth conditions were 0.02M, 75º C for 75 minutes on Ag substrate.

In conclusion, three different substrates (Au, Al, and Ag) were used, while varying the temperature, deposition time and the concentration of zinc nitrate and methenamine in the solution. Each substrate allowed for the growth of ZnO nanorods, but in directions and planes that were not optimal for the future of this research. The most promising results were obtained using a Ag substrate, a 0.02 equimolar solution, at 75º C for a 75 minute deposition time. The rods shown

above in Figures 3.23 and 3.24 show promise in that an electrical contact using a 2-point probe system can be made.

X-ray diffraction was also performed on the specimen shown in Figure 3.23 to confirm that ZnO is present. The data is shown below in Figure 3.25. Peaks 3 and 9, labeled on the graph, are consistent with ZnO <002> and <200> peaks, respectively. Other features can be attributed to the Ag and Si substrate. The peaks appear to not be very strong peaks, which can be attributed to the small amount of ZnO deposited.

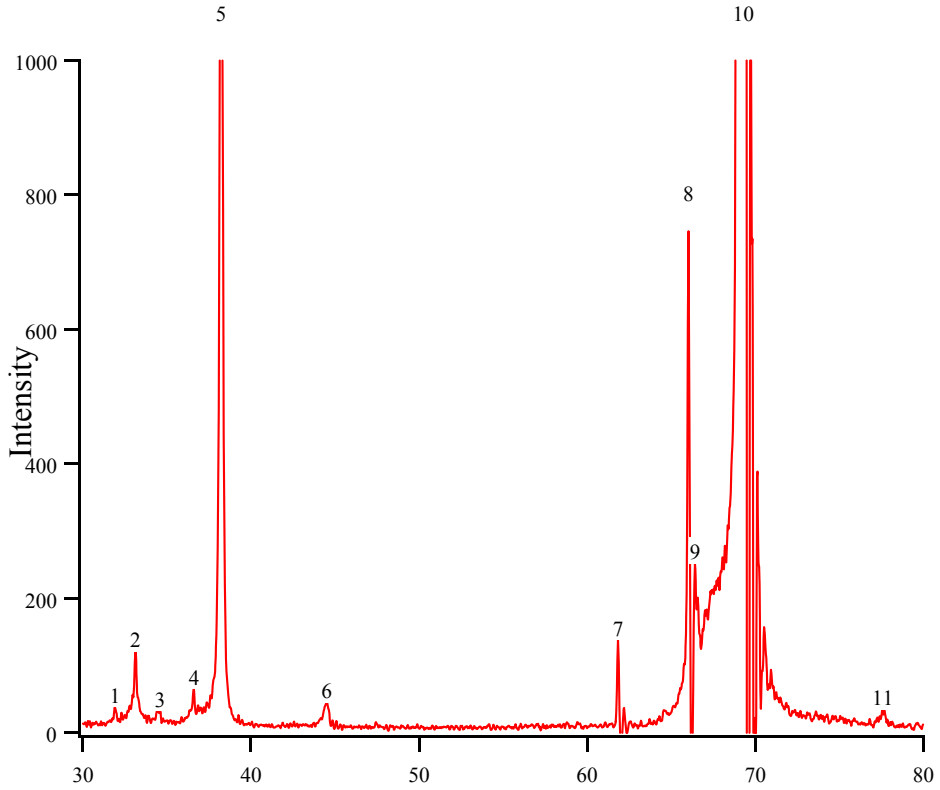

Figure 3.25 Symmetric XRD of ZnO Wet Chemistry Sample 016

CHAPTER 4

CONCLUSION AND FUTURE WORK

4.1 Conclusion

Zinc Oxide is a wide band gap, group II-VI semiconductor with several interesting properties. One of its most important properties is its piezoelectricity, which would allow the electrical properties to be coupled to mechanical performance. In the semiconductor industry, as devices are getting smaller in size, the need for specific nanostructures increases. This is the reason ZnO nanorods may be very necessary for the future of electronic materials and devices.

The research described here in the previous chapters encompasses two different deposition methods, electrodeposition and wet chemistry. The first method explored was electrodeposition. ZnO was deposited in the hexagonal structure. However, ZnO nanorods or columns were not grown; only platelets were found. Concentration of electric field at the edges of the platelets appeared to yield the observed growth form. If further experiments are to be done using electrodeposition, then a possible increase in the molarity of the $ZnCl_2$, above 0.05M, should be studied.

Next, wet chemistry was examined as a possible method to deposit the desired ZnO nanorods. This deposition method showed great promise for the

progression of this research project. And, after exploring three different substrates (Au, Al and Ag), different molarities of concentration (0.02M and 0.1M), for various deposition times and temperatures, ZnO hexagonal nanorods were grown, perpendicular to the substrate with growth along the (0001) plane. The Ag substrate gave the best results.

Given the limited time, best results were obtained with wet chemical growth. However, results elsewhere [7, 8] and initial results here suggest that electrochemistry might be used to deposit nano-scaled structures.

Lastly, the exact cause of nucleation was not investigated for these experiments. It is unknown whether contamination, such as that occurring during evaporation of the substrate or oxidation of the substrate, has had any impact on the growth. In Hsu's research [10], it is shown that self-assembled monolayers helped inhibit the growth of ZnO in specific areas on the surface, so that growth could be isolated. The various substrates resulted in different growth structures of ZnO. The mechanism for growth and nucleation for these experiments needs to be determined so that growth can be controlled. In the future, since the optimal parameters were identified, a closer observation of the cause of nucleation must be examined.

4.2 Future Work

As stated previously, the next step to take in this research is to deposit a thin insulating layer of SiO_2 using Plasma Enhanced Chemical Vapor Deposition (PECVD). The Samco PD-220N plasma CVD will be used to deposit a layer that is approximately 700Å; the purpose of this layer is to isolate the semi conductivity of each ZnO nanorods on the surface before making an electrical contact.

Next, Focused Ion Beam (FIB) technology will be used to mill holes through the SiO_2 layer to make an electrical contact with the ZnO nanorods. The FIB located at Penn State University will be used. A dual beam FIB combines SEM and FIB into one machine, for the analysis of structure below 100 nm in size. As mentioned previously, the SEM uses an electron beam, while the FIB uses a fine focused beam of Ga^+ ions, instead of electrons. The Ga^+ beam is rastered onto the surface of the material; as it hits the surface, a small amount of material is removed from the surface. And, the higher the primary beam current, the more material will be sputtered or removed from the surface. The FIB will be used in high-beam operation because this mode is intended for removing material from the surface, for example, during high-precision milling. Also, a FIB system is capable of bombarding an area with various gases as it performs primary beam sputtering. Depending on what gases are used, they can react with the primary Ga^+ beam to

either etch material or deposit material on the surface. After drilling the holes through the SiO2, a metal will need to be deposited for the electrical contact.

After milling holes via Focused Ion Beam through the insulating layer of SiO_2, a two point or four point electrical probe system will be used to gather information about the ZnO nanorods. For a simple electrical resistance measurement, the two point probe, which utilizes Ohm's Law (R=V/I), can be applied. However, a concern with the two point probe is that the contact resistance, the resistance at the contact points of the probes, is also measured. If the contact resistance is much less than the resistance of the sample, it becomes negligible. But, if the sample being measured has a very small resistance, the contact resistance may dominate and cause changes in the resistance to become obscure. Thus, a four point probe system may be more useful; and, the contact resistance can be eliminated. Also, the four point probe will give a more accurate I-V curve, because the second set of probes is used for sensing. Since negligible current flows in these probes, only the voltage drop across the area being tested is measured.

Shown below is a schematic diagram of the next few steps of this research.

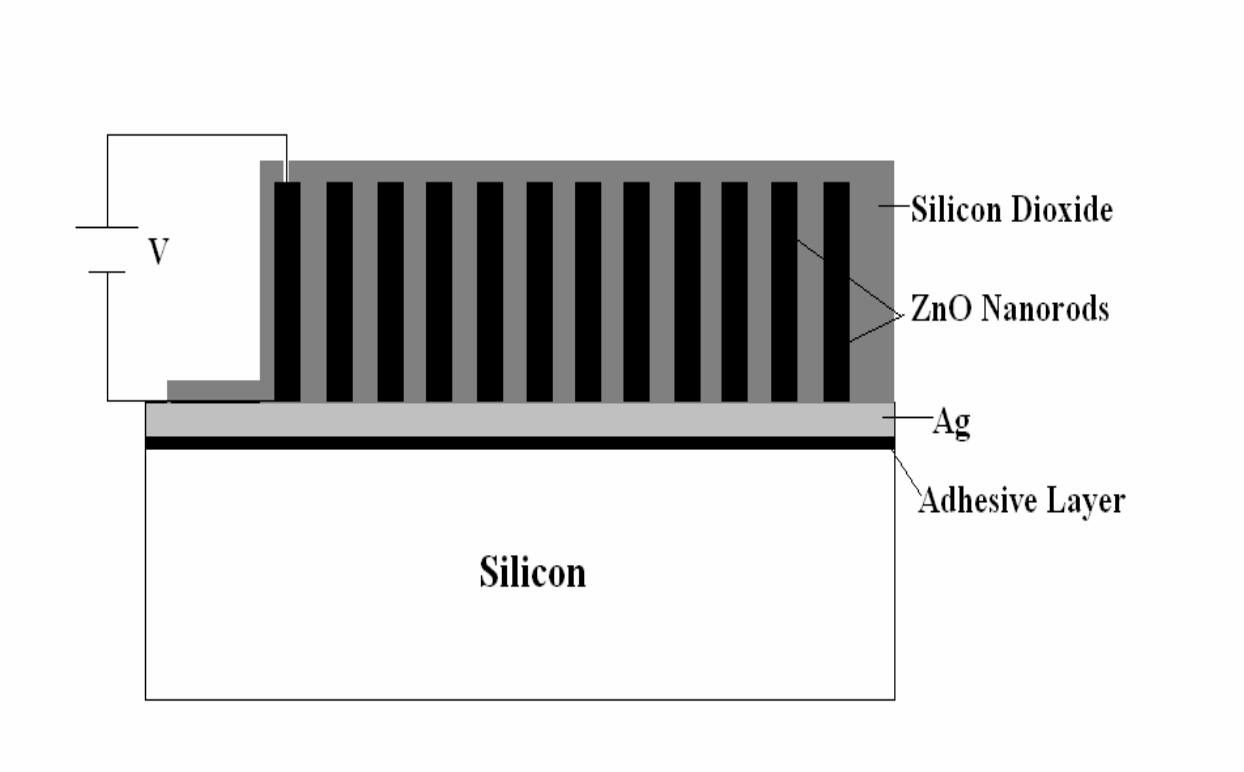

Figure 4.1 Schematic of future work using a two point probe

BIBLIOGRAPHY

[1] D.P. Norton and S. J. Pearton, Applied Physics Letters 82, 239 (2003)

[2] Zhang Lin Wang, Materials Today 7, 26 (2004)

[3] Zhang Lin Wang, Journal of Physics: Condensed Matter 16, R829 (2004)

[4] Xiang Yang and Zhang Lin Wang, Nano Letter 3, 1623 (2003)

[5] Michael H. Huang, Samuel Mao, Henning Feick, Haoquan Yan, Yiying Wu, Hannes Kind, Eicke Weber, Richard Russo, and Peidong Yang, Science 292, 1897 (2001)

[6] D.P. Norton, Y. W. Heo, M. P. Ivill, K. lp, S. J. Pearton, M.F. Chisholm, and T. Steiner, Materials Today 7, 34 (2004)

[7] Masanobu Izaki and Takashi Omi, Applied Physics Letters 68, 2439 (1996)

[8] Run Liu, Alexey A. Vertegel, Eric W. Bohannan, Thomas A. Sorenson, and Jay A. Switzer, Chemistry of Materials 13, 508 (2001)

[9] Sophie Peulon and Daniel Lincot, Advanced Material 8, 166 (1996)

[10] Julia W. P. Hsu, Zhengrong R. Tian, Neil C. Simmons, Carolyn M. Matzke, James A. Voigt, and Jun Liu, Nano Letters 5, 83 (2005)

[11] Lionel Vayssiers, Karin Keis, Sten-Eric Lindquist, and Anders Hagfeldt, Journal of Physical Chemistry B 105, 3350 (2001)

[12] Julia W.P. Hsu, Zhenrong R. Tian, Neil C. Simmons, Carolyn M. Matzke, James A. Voigt, and Jun Liu, The International Society for Optical Engineering 5592, 158 (2005)

[13] Daniel Lincot, Thin Solid Films 487, 40 (2005)